

# Mg-Al Mixed Oxides Supported Bimetallic Au-Pd Nanoparticles with Superior Catalytic Properties in Aerobic Oxidation of Benzyl Alcohol and Glycerol<sup>†</sup>

Wang, Liang<sup>b</sup>(王亮)    Zhang, Wei<sup>c</sup>(张伟)    Zeng, Shangjing<sup>b</sup>(曾尚景)  
Su, Dangsheng<sup>\*c</sup>(苏党生)    Meng, Xiangju<sup>a</sup>(孟祥举)    Xiao, Fengshou<sup>\*a</sup>(肖丰收)

<sup>a</sup> Key Lab of Applied Chemistry of Zhejiang Province, Department of Chemistry, Zhejiang University, Hangzhou, Zhejiang 310028, China

<sup>b</sup> State Key Laboratory of Inorganic Synthesis and Preparative Chemistry, Jilin University, Changchun, Jilin 130012, China

<sup>c</sup> Department of Inorganic Chemistry, Fritz Haber Institute of the Max Planck Society, Faradayweg 4-6, Berlin 14195, Germany

Nano-sized Au and Pd catalysts are favorable for oxidations with molecular oxygen, and the preparation of this kind of nanoparticles with high catalytic activities is strongly desirable. We report a successful synthesis of bimetallic Au-Pd nanoparticles with rich edge and corner sites on unique support of Mg-Al mixed oxides (Au-Pd/MAO), which are favorable for producing metal nanoparticles with high degree of coordinative unsaturation of metal atoms. The systematic microscopic characterizations confirm the bimetallic Au-Pd nanoparticles are present as Au-Pd alloy. The irregular shape of the bimetallic nanoparticles are directly observed in HRTEM images. As we expected, Au-Pd/MAO gives very excellent catalytic performances in the aerobic oxidation of benzyl alcohol and glycerol. For example, Au-Pd/MAO shows very high TOF of 91000 h<sup>-1</sup> at 433 K with molecular oxygen at air pressure in solvent-free oxidation of benzyl alcohol; this catalyst also shows relatively high selectivity for tartronic acid (TA-RAC, 36.6%) at high conversion (98.5%) in aerobic oxidation of glycerol. The superior catalytic properties of Au-Pd/MAO would be potentially important for production of fine chemicals.

**Keywords** bimetallic Au-Pd nanoparticles, Mg-Al mixed oxides, selective oxidation, benzyl alcohol, glycerol, molecular oxygen

## Introduction

Supported Au, Pd or Au-Pd nanoparticles have attracted much interest owing to their unusual catalytic performances, especially for the oxidations.<sup>[1-20]</sup> The catalytic performances of Au or Pd nanoparticles are highly related to their particle size and morphology.<sup>[21,22a]</sup> Usually, Au or Pd nanoparticles with small size and irregular shape can give high catalytic activities for oxidations, because they have a large number of metal atoms on the facet-edge and corner positions, which are regarded as active sites for binding or dissociation of molecular oxygen.<sup>[21-23]</sup> Recently, the search for effective methodology to synthesize Au or Pd nanoparticles with high degree of coordinative unsaturation of metal atoms is a hot topic. One attractive approach is to synthesize small metal nanoparticles on unique metal oxides, because the morphology of metal

nanoparticles is strongly dependent on the metal oxide supports.<sup>[21,24,25]</sup> For example, Au nanoparticles supported on Fe<sub>2</sub>O<sub>3</sub> show flat morphology, exhibiting a good performance for dissociation of molecular oxygen.<sup>[25]</sup> More recently, it is reported that the formation of bimetallic alloys is favorable for creation of irregular morphology of the nanoparticles. For example, bimetallic Au-Pd nanoparticles with twined structure on carbon support exhibit excellent catalytic properties for oxidations.<sup>[26,27]</sup>

As a typical model of oxidations, catalytic conversions of benzyl alcohol by molecular oxygen have already been investigated with Au, Pd and Au-Pd nanoparticles supported on solids like polymers, hydroxyapatite, hydrotalcite, silica, carbon, and metal oxides.<sup>[6,11,17,26,27]</sup> For example, Kaneda and co-workers reported that Pd nanoclusters on hydroxyapatite is very active for oxidation of benzyl alcohol with

\* E-mail: dangsheng@fhi-berlin.mpg.de; fsxiao@mail.jlu.edu.cn; Tel.: 0086-0431-85168590

Received March 19, 2012; accepted May 9, 2012; published online XXXX, 2012.

Supporting information for this article is available on the WWW under <http://dx.doi.org/10.1002/cjoc.201200271> or from the author.

<sup>†</sup> Dedicated to the 80th Anniversary of Chinese Chemical Society.

high yield of benzaldehyde at 99%;<sup>[11]</sup> Cao and co-workers found that Au nanoparticles on Ga-Al mixed oxides give 98% conversion of benzyl alcohol to benzaldehyde.<sup>[9]</sup> These catalysts are highly active, but organic solvents were used in most of these cases. Very interestingly, Hutchings and co-workers reported the successful oxidation of phenyl alcohol over TiO<sub>2</sub> supported bimetallic Au-Pd nanoparticles in the absence of organic solvents, with a quite high turnover frequency (TOF) as high as 86500 h<sup>-1</sup>.<sup>[28]</sup>

On the other hand, glycerol is a major by-product in the production of biodiesel from transesterification and its supply is increasing in these years.<sup>[29,30]</sup> Considering of its highly functional abilities, the selective oxidation of glycerol is an alternative route to increase its value, because the products such as glyceric acid (GLYA) and tartronic acid (TARAC) are important intermediates for the production of fine chemicals and medicine.<sup>[31]</sup> The oxidation of glycerol by molecular oxygen has already been performed on various metals (Au, Pt-Bi, Au-Pd) supported on carbon and metal oxides.<sup>[4,27,32-34]</sup> The activities and product selectivities of this reaction strongly depend on the reaction conditions and catalyst structure (metal, support, and particle size). Notably, despite of very successful catalytic oxidation of glycerol in recent years, it is still a challenge for obtaining high selectivities for desired products (*e.g.* GLYA, TARAC) at high glycerol conversion because of the side reaction of C-C bond scission.<sup>[35,36]</sup>

We demonstrate here a design and preparation of bimetallic Au-Pd nanoparticles with rich edge and corner sites on Mg-Al mixed oxides (molar ratio of Mg/Al at 3). This kind of catalysts shows superior catalytic performances in aerobic oxidations of benzyl alcohol and glycerol, compared with the catalysts reported previously.

## Experimental

For the preparation of 0.7% Au-0.9% Pd/MAO, (1) 30.76 g of Mg(NO<sub>3</sub>)<sub>2</sub>·6H<sub>2</sub>O and 15 g Al(NO<sub>3</sub>)<sub>3</sub>·9H<sub>2</sub>O were dissolved in 400 mL of water, followed by addition of 72 g of urea under stirring. After boiling for 8 h, precipitating at room temperature for 12 h, filtrating and washing with large amount of water, the sample obtained was designated as Mg-Al double hydroxide (LDH, molar ratio of Mg/Al at 3); (2) 10 g of Mg-Al double hydroxide was added into a solution of HAuCl<sub>4</sub> and Na<sub>2</sub>PdCl<sub>4</sub> (1 mmol Pd and 0.4 mmol Au) and stirred at room temperature for 8 h. After filtrating, washing with a large amount of water, and drying at room temperature overnight, the obtained solid (Au-Pd/MAO) was treated at 373 K for 6 h and 673 K for 3 h. Au and Pd loadings were analyzed by inductively coupled plasma spectroscopy (ICP). 0.7% Au/MAO or 0.9% Pd/MAO was obtained by adjusting the Au or Pd content.

For the preparation of 1.3% Au/SBA-15, SBA-15 was synthesized and coated by *N*-[3-(trimethoxysilyl)-

propyl]diethylenetriamine (DETA) according to literature.<sup>[34]</sup> The DETA coated SBA-15 was stirred in HAuCl<sub>4</sub> solution overnight. The product was collected, dried at room temperature, and calcined at 673 K for 3 h. The Au loading (1.3 wt%) was analyzed by ICP.

As a typical run for the preparation of MgO, 30.76 g of Mg(NO<sub>3</sub>)<sub>2</sub>·6H<sub>2</sub>O was dissolved in 400 mL of water, followed by addition of 72 g of urea under stirring. After boiling for 8 h, precipitating at room temperature for 12 h, filtrating and washing with large amount of water, drying at room temperature overnight, the obtained solid was treated at 373 K for 6 h and 673 K for 3 h, giving white sample of MgO. Similarly, we prepared Al<sub>2</sub>O<sub>3</sub>.

2.2% Au/CeO<sub>2</sub> and 0.2% Pd/HAP catalysts were synthesized according to literature.<sup>[6,11]</sup> For the preparation of 0.5% Au-0.6% Pd/SiO<sub>2</sub>, 2.0 g of 0.7% Au-0.9% Pd/MAO and 1 g of SiO<sub>2</sub> were added to 20 mL of water, followed by the addition of HCl (1.0 mol/L) and stirring at room temperature for 8 h. After filtration and calcination at 673 K for 3 h, the solid sample was washed with HCl (0.5 mol/L) to remove the Mg and Al species. The Au and Pd loadings were 0.5 wt% and 0.6 wt%, respectively.

Powder X-ray diffraction patterns (XRD) were obtained with a Siemens D5005 diffractometer and Rigaku D/MAX 2550 diffractometer with Cu K $\alpha$  radiation ( $\lambda = 0.1542$  nm). The BET surface area was measured using a Micromeritics ASAP Tristar. The samples were outgassed for 10 h at 150 °C before the measurement. A FEI Titan 80-300 microscope was employed to conduct microscopy and analyses of the samples in both transmission electron microscopy (TEM) and scanning transmission electron microscopy (STEM) modes, operating at 300 kV. An EDX detector is equipped to the microscope for the analysis of chemical compositions. The content of metal was determined from inductively coupled plasma (ICP) with a Perkin-Elmer plasma 40 emission spectrometer. Temperature programmed surface reaction (TPSR) of adsorbed 2-propanol was carried out as follows: the catalysts were treated at 573 K for 3 h and cooled down to room temperature, then 2-propanol vapor was introduced into the reaction system for 30 min. After sweeping with Ar for 1 h, the temperature was increased (10 K/min) from room temperature to 773 K, and the signals of H<sub>2</sub> were recorded by mass spectrometer with a thermal conductivity detector (TCD). XPS spectra were performed by a Thermo ESCALAB 250, and the binding energies were calibrated by C1s peak (284.9 eV). Typical for the characterization of NH<sub>3</sub>-TPD, CO<sub>2</sub>-TPD, and H<sub>2</sub>-TPR, the sample loaded in a quartz reactor was pretreated with high pure He at 400 °C for 1 h. The temperature was increased at the rate of 10 °C/min. A ThermoStar GSD mass spectrometer was used to detect the signal.

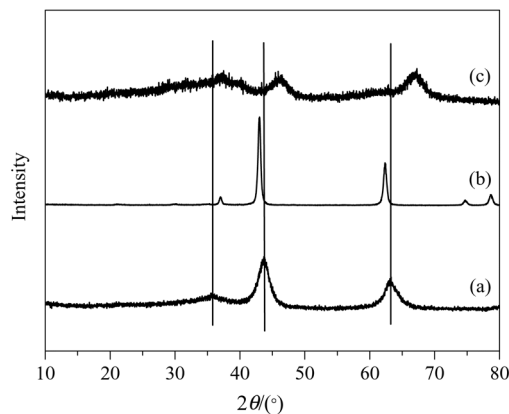
Benzyl alcohol and glycerol oxidations were performed in a 100 mL autoclave with a magnetic stirrer. Typically, substrate, solvent, and catalyst were mixed in the reactor, then the mixture was stirred (1200 r/min).

After increasing temperature (the temperature was measured with a thermometer in an oil bath), molecular oxygen was introduced to the reaction system and kept at desired pressure. After the reaction, the benzyl alcohol oxidation products were analyzed by gas chromatography (GC-14C, Shimadzu, FID) with a flexible quartz capillary column of FFAP, and the glycerol oxidation products were analyzed by gas chromatography (GC-14C, Shimadzu) with a flexible quartz capillary column of OV-17 and high-pressure liquid chromatograph (HPLC, Bruker) equipped with a column of OA-10308.  $\text{H}_3\text{PO}_4$  solution (0.1%) was used as the eluent. The recyclability of the catalyst was tested by separating it from the reaction system by centrifugation, washing with large quantity of methanol and drying at 373 K for 6 h, then the catalyst was reused in the next reaction. The turnover frequency (TOF) in the oxidation of benzyl alcohol over Au-Pd/MAO catalyst was calculated from the converted benzyl alcohols per metal atom (total metal loading) and hour. The converted benzyl alcohols were determined at 433 K under an atom spherical oxygen, reaction time for 0.5 h, 250 mmol of benzyl alcohol, and 10 mg of catalyst.

## Results and discussion

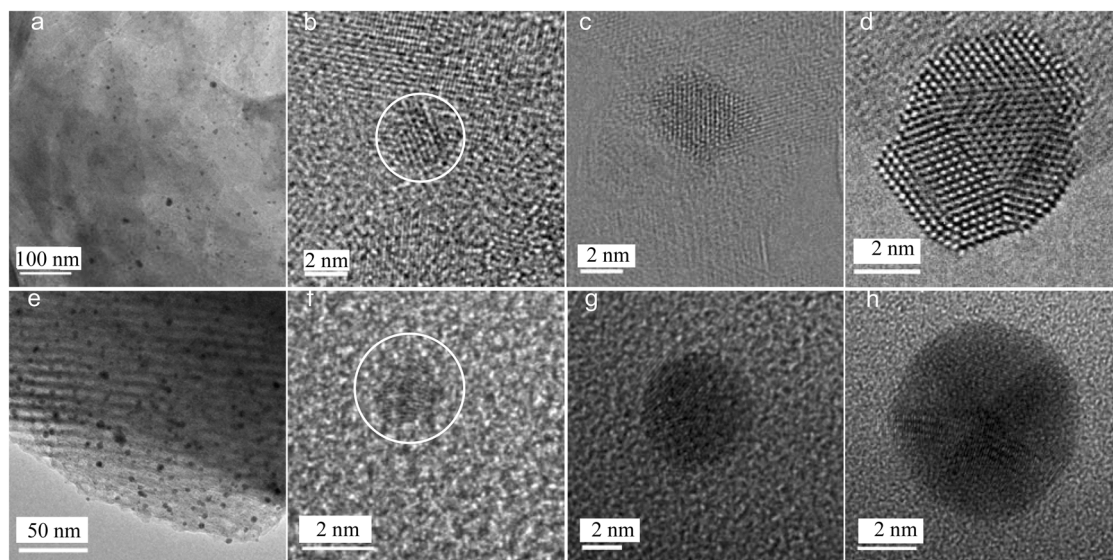
Figure 1 shows the XRD patterns of various oxides. MAO shows three peaks at  $35.7^\circ$ ,  $43.8^\circ$  and  $63.2^\circ$  (Figure 1a), indicating that the layered structure of LDH is destroyed during the calcination process. However, the surface area of MAO increases to  $75.0 \text{ m}^2/\text{g}$  from  $66.3 \text{ m}^2/\text{g}$  for LDH. Notably, the three peaks could not be found on the XRD pattern of MgO or  $\text{Al}_2\text{O}_3$  self (Figure 1b and 1c). These results suggest that MAO is not a simple mixture of MgO and  $\text{Al}_2\text{O}_3$ .

Figure 2 shows TEM images of 0.7% Au/MAO and 1.3% Au/SBA-15, demonstrating that the Au nanoparticles with similar size distributions on both samples are



**Figure 1** XRD patterns of (a) MAO, (b) MgO and (c)  $\text{Al}_2\text{O}_3$ .

highly dispersed on MAO or in the mesoporous of SBA-15. High-resolution TEM images exhibit that the morphology of Au nanoparticles with very similar sizes over MAO or mesoporous SBA-15 support is quite different. In contrast to the Au nanoparticles of 1.3% Au/SBA-15, which are rounded in shape, those of 0.7% Au/MAO exhibit much more faceted and angular features, giving rich facet-edge and corner Au atoms. In order to investigate the origin of the different morphology of Au nanoparticles, Au4f XPS spectra of both samples were shown in Figure 3. 1.3% Au/SBA-15 gives binding energy of Au4f<sub>7/2</sub> at 84.0 eV, which is attributed to typical metallic Au.<sup>[17]</sup> Interestingly, 0.7% Au/MAO gives binding energy of Au4f<sub>7/2</sub> at 84.5 eV, with 0.5 eV of shift from 1.3% Au/SBA-15, suggesting the Au nanoparticles on MAO are positively charged.<sup>[21]</sup> Furthermore, the  $\text{H}_2$ -TPR profiles of MAO and Au/MAO are shown in Figure 4. Both samples have no signals at the temperature lower than  $350^\circ\text{C}$ , indicating that the Au species of Au/MAO are present as metallic Au, instead of  $\text{Au}^+$  or  $\text{Au}^{3+}$  cations.<sup>[22b]</sup> The peaks at



**Figure 2** (a) TEM, particle size distribution and (b–d) HRTEM images of 0.7% Au/MAO; (e) TEM, particle size distribution and (f–h) HRTEM images of 1.3% Au/SBA-15.

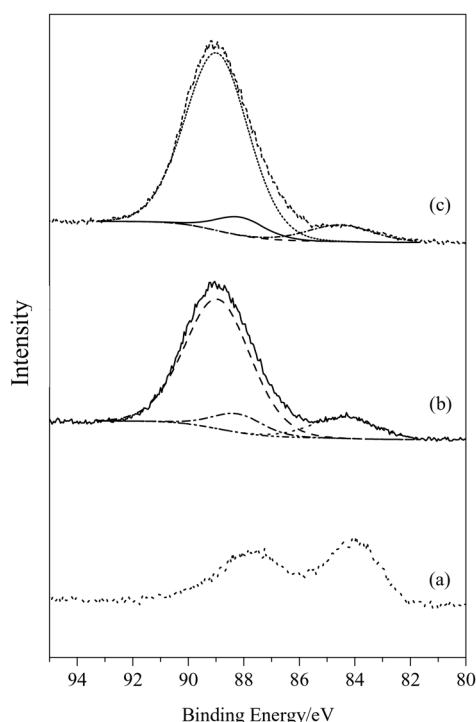


**Figure 3** Au4f XPS spectra of (a) 1.3% Au/SBA-15, (b) 0.7% Au/MAO and (c) 0.7% Au-0.9% Pd/MAO.

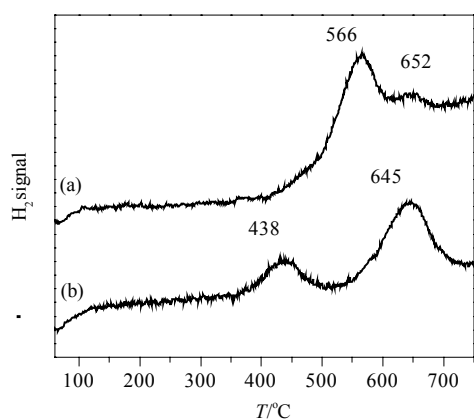


**Figure 4** H<sub>2</sub>-TPR profiles of (a) MAO and (b) Au/MAO.

566 and 652 °C for MAO sample are attributed to the reduction of surface oxygen species of MAO, while this kind of signal appeared on the profile of Au/MAO as a peak at 645 °C with strong intensity. This might originate from the interaction between Au nanoparticles and MAO support. Additionally, Au/MAO sample shows another reduction peak at lower temperature of 438 °C, this might be due to the weakening of the Mg—O or Al—O bond by strongly bound Au species.<sup>[22c,22d]</sup> These results indicate that the Au species are present as metallic Au on Au/MAO, and there is strong interaction between Au species and MAO support, which highly agrees with the results obtained from the XPS spectra. In consideration of the similar Au particle size of 0.7%

Au/MAO and 1.3% Au/SBA-15, this shift in binding energy is reasonably assigned to the interaction between Au nanoparticles and MAO support. By this interaction, Au nanoparticles tend to form an extended flat interface structure with the support.<sup>[21]</sup> Possibly, the crystalline MAO substrate directs the formation of Au nanoparticles with rich edge and corner Au atoms in 0.7% Au/MAO. In contrast, amorphous SBA-15 does not have this kind of ability to direct the formation of Au nanoparticles with irregular morphology. These results suggest that MAO is a suitable support for forming Au nanoparticles with rich edge and corner sites.

In consideration of the directing ability of MAO support, the investigation on bimetallic Au-Pd nanoparticles on MAO is desirable. Energy dispersive X-ray analyses (EDX) of particles indicate the presence of both Au and Pd atoms in one single particle, and the ratios of Au to Pd are almost unchanged for the examined particles (Figure 5). Additionally, STEM images (Figures 6a, 6e and 6i) demonstrate that the Au, Pd or Au-Pd nanoparticles are highly dispersed on the MAO support. Compared to monometallic nanoparticles, bimetallic ones exhibit a much smaller size distribution (Figures 6b, 6f and 6j). HRTEM images of various metal nanoparticles with similar particle size of 2 nm (Figures 6c, 6g and 6k) show that the bimetallic Au-Pd nanoparticles (Figure 6k) provide quite different lattice spacings as compared to pure Au (Figure 6c) or Pd nanoparticles (Figure 6g). The Au-Pd nanoparticle with a twined boundary has the lattice spacing of 0.232 nm for the {111} plane, which locates between 0.239 nm for {111} Au and 0.223 nm for {111} Pd. Fast Fourier Transform (FFT) analysis shows that the Au-Pd nanoparticle is a typical twin, and each part has a FCC structure (Figure 6l), similar to Au or Pd nanoparticle (Figures 6d and h). These results indicate that Au-Pd nanoparticles are alloys rather than separated phases of Au or Pd. The formation of Au-Pd alloy leads to the change in the lattice spacing, therefore giving the difference in electronic structure,<sup>[27,37]</sup> even if there is no electron transfer between Au and Pd species. This phenomenon is confirmed by the fact that both 0.7% Au/MAO and 0.7% Au-0.9% Pd/MAO give similar binding energy of Au4f<sub>7/2</sub> at 84.5 eV in the Au4f XPS spectra (Figure 3). Figures 6m—6r show HRTEM images of Au-Pd nanoparticles with different sizes. Most of Au-Pd nanoparticles have clear boundaries, which are quite distinguishable from monometallic Au or Pd nanoparticles. In particular, as observed in Figures 6q and 6r, the Au-Pd nanoparticles have more than ten boundaries. This kind of special boundary structure could produce a large amount of low-coordinative facet-edge and corner sites, which could be favorable for oxidation reactions.<sup>[21,23,37]</sup> Additionally, in the Au-Pd alloy, one metal acts as promoter to isolate monomer sites of another metal, which could be helpful for improving the catalytic activities.<sup>[16]</sup>

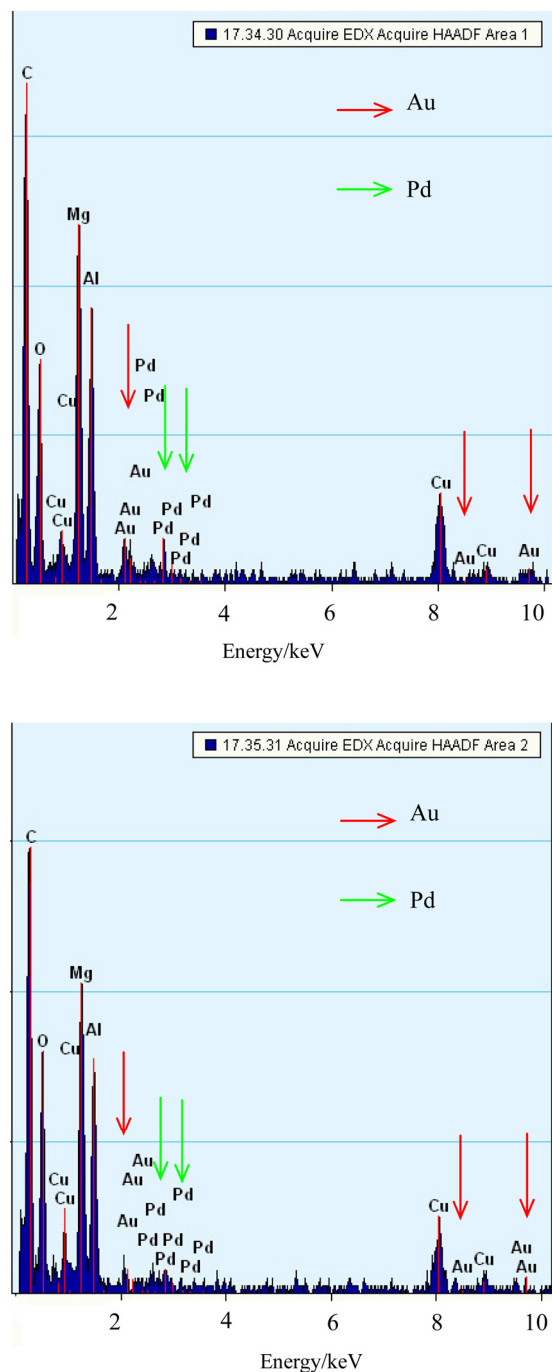


**Figure 5** EDX spectra of individual single nanoparticle of 0.7% Au-0.9% Pd/MAO.

In liquid phase oxidations, the oxidation of benzyl alcohol to benzaldehyde was chosen as a test reaction since the selective formation of benzaldehyde can be challenged by a number of possible side-reactions such as hydrogenolysis, decarbonylation, and esterification.<sup>[26,38]</sup> Catalytic data of solvent-free aerobic oxidation of benzyl alcohol over Au, Pd and Au-Pd catalysts are presented in Table 1. 0.7% Au/MAO and 0.9% Pd/MAO catalysts show a conversion of 21.2% and 11.2% and a selectivity to benzaldehyde of 54.2% and 40.9%, respectively (Table 1, Entries 1 and 2). However, 0.7%

Au-0.9% Pd/MAO catalyst shows a drastically improved catalytic performance at a conversion and selectivity of 95.4% and 83.5% (Table 1, Entry 3). Contrarily, a physical mixture of 0.7% Au/MAO and 0.9% Pd/MAO shows a low conversion of 24.3% and selectivity of 44.5% (Table 1, Entry 4). These results suggest a synergy between Au and Pd in terms of catalytic activity when forming bimetallic Au-Pd nanoparticles supported on MAO. Notably, 0.7% Au-0.9% Pd/MAO is even more active than the hydroxyapatite supported Pd catalyst (Pd/HAP) and the ceria supported Au catalyst (Au/CeO<sub>2</sub>, Table 1, Entries 5 and 6), which represent two of the most active catalysts for aerobic oxidation of alcohols reported so far.<sup>[6,11]</sup> The silica supported 0.5% Au-0.6% Pd/SiO<sub>2</sub> shows a conversion of 67.0% at a selectivity of 88.2% (Table 1, Entry 7). Considering the similar size and structure of bimetallic Au-Pd nanoparticles on SiO<sub>2</sub> and MAO supports, higher activity over 0.7% Au-0.9% Pd/MAO than 0.5% Au-0.6% Pd/SiO<sub>2</sub> suggests a strong influence of the support on the activity.

**Table 1** Catalytic data in solvent-free aerobic oxidation of benzyl alcohol over Au, Pd and Au-Pd catalysts<sup>a</sup>

Entry	Catalyst	Conversion of benzyl alcohol/%	Selectivity to benzaldehyde <sup>b</sup> /%
1	0.7% Au/MAO	21.2	54.2
2	0.9% Pd/MAO	11.2	40.9
3	0.7% Au-0.9% Pd/MAO	95.4	83.5
4	0.7% Au/MAO+0.9% Pd/MAO <sup>c</sup>	24.3	44.5
5	0.2% Pd/HAP	60.7	39.5
6	2.2% Au/CeO <sub>2</sub>	19.1	95.7
7	0.5% Au-0.6% Pd/SiO <sub>2</sub> <sup>d</sup>	67.0	88.2
8	0.7% Au-0.9% Pd/MAO <sup>e</sup>	88.0	72.4
9	0.7% Au-0.9% Pd/MAO <sup>f</sup>	94.0	81.0

<sup>a</sup> Reaction conditions: 80 mg catalyst, 30 mmol substrate, 0.2 MPa O<sub>2</sub>, 373 K, reaction time for 7 h; dodecane was used as internal standard and the benzaldehyde productivity was calculated for the reaction time at 7 h; <sup>b</sup> The by-products are major benzyl benzoate, benzoic acid, and toluene; <sup>c</sup> Physical mixture of 40 mg 0.7% Au/MAO with 40 mg 0.9% Pd/MAO; <sup>d</sup> 110 mg catalyst; <sup>e</sup> 0.4 MPa air and reaction time for 11 h; <sup>f</sup> Recycles for 5 times.

To understand the role of MAO support, the dehydrogenation test of the MAO support for adsorbed isopropanol was carried out (Figure 7). The choice of 2-propanol is due to its relatively low boiling point. Interestingly, it is observed strong signals associated with hydrogen on MAO support. This suggests that the MAO support has a strong dehydrogenation ability, which is a key step in alcohol oxidations and could be important for enhancing activities in these oxidations.<sup>[32a]</sup> In contrast, silica and TiO<sub>2</sub> support has no dehydrogenation ability.<sup>[39]</sup> Furthermore, CO<sub>2</sub>-TPD was performed to

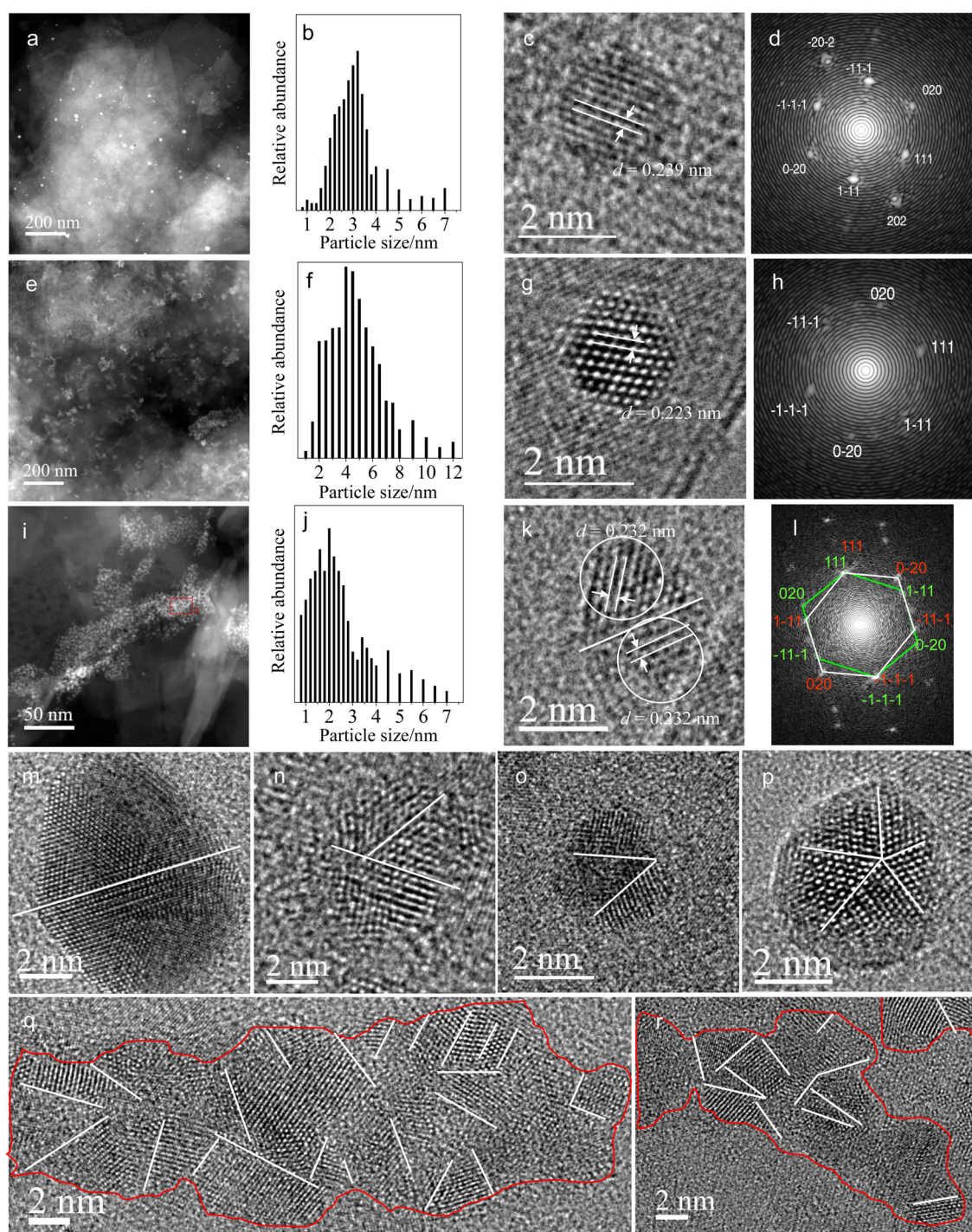


**Figure 6** (a) STEM image, (b) particle size distribution, (c) HRTEM image, and (d) FFT analysis of 0.7% Au/MAO; (e) STEM image, (f) particle size distribution, (g) HRTEM image, and (h) FFT analysis of 0.9% Pd/MAO; (i) STEM image, (j) particle size distribution, (k and m–r) HRTEM images, (l) FFT analysis of 0.7% Au-0.9% Pd/MAO. The white lines mark the boundary.

investigate the origin of dehydrogenation ability of MAO (Figure 8). The profile of  $\text{CO}_2$ -TPD shows obvious peak at the temperature of 560 °C, indicating the strong basicity of MAO support. While  $\text{SiO}_2$  support does not have any basic peaks according to the reported literature.<sup>[32b]</sup> The basicity is helpful for the dehydrogenation ability, and these results highly agree with those

obtained from the dehydrogenation test. Additionally, in the profile of  $\text{NH}_3$ -TPD, MAO also gives obvious peaks at 145 and 594 °C, indicating its strong acidity. According to the previous literature, the strong basicity could afford higher activity and the strong acidity could afford high selectivity for aldehyde for the oxidation of alcohols.<sup>[32b]</sup>

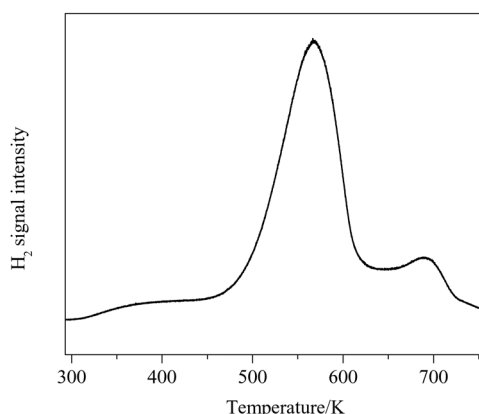


Figure 7 TPSR spectrum of 2-propanol adsorbed on MAO.

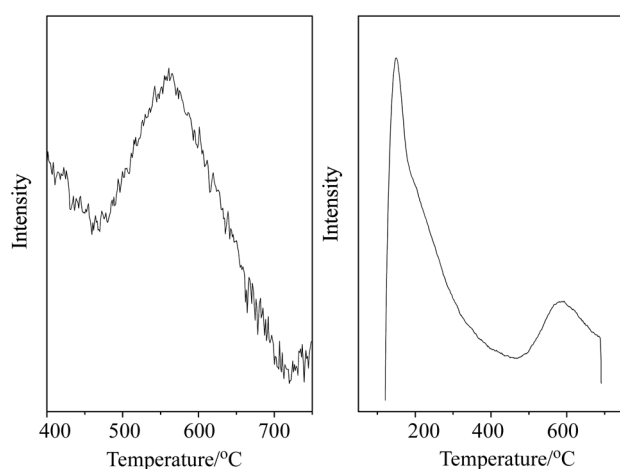


Figure 8 (left) CO<sub>2</sub>-TPD and (right) NH<sub>3</sub>-TPD profiles for MAO.

In addition, using air as the source of O<sub>2</sub>, 0.7% Au-0.9% Pd/MAO still shows the high conversion of 88.0% and selectivity of 72.4%, which is an economically important factor for industrial applications (Table 1, Entry 8). After 5 times of catalyst recycling 0.7% Au-0.9% Pd/MAO catalyst is still very active, ending up at the conversion of 94.0% and selectivity of 81%, which in-

dicates its excellent recyclability (Table 1, Entry 9). At the same time, ICP analysis of the liquid collected from the reaction mixture proves the absence of Au and Pd species, indicating that metal-leaching is negligible under the reaction conditions applied.

The TOF for the solvent-free oxidation of benzyl alcohol at 433 K under 0.1 MPa O<sub>2</sub> is 86500 h<sup>-1</sup> as reported by Hutchings and co-workers,<sup>[28]</sup> which is a very high value. 0.7% Au-0.9% Pd/MAO shows an even higher TOF of 91000 h<sup>-1</sup> at 433 K with molecular oxygen at air pressure. These data confirm that 0.7% Au-0.9% Pd/MAO is very active for oxidation of benzyl alcohol.

As the simplest triol in nature, oxidation of glycerol is greatly significant for the conversion of biomass. Table 2 presents the catalytic activities in glycerol oxidation with molecular oxygen over various Au, Pd and Au-Pd catalysts. 0.7% Au/MAO and 0.9%Pd/MAO catalysts show similar TOFs at 1840–2300 h<sup>-1</sup> (Table 2, Entries 1 and 2). Very interestingly, 0.7% Au-0.9% Pd/MAO catalyst gives a drastically improved catalytic activity, giving TOF at 9200 h<sup>-1</sup> (Table 2, Entry 3). This value is even higher than that (TOF at 6435 h<sup>-1</sup>, Table 2, Entry 4) of Au-Pd nanoparticles on active carbon under similar conditions, a very successful example for glycerol oxidation.<sup>[27]</sup> Furthermore, it is worth noting that both 0.7% Au/MAO and 0.7% Au-0.9% Pd/MAO catalysts are catalytically active in absence of NaOH, giving TOF at 1100 and 2820 h<sup>-1</sup>, respectively (Table 2, Entries 7 and 8). This phenomenon is quite different from the results reported in literature that no reaction occurred on most of Au catalysts without addition of bases.<sup>[15]</sup> Possibly, the strong dehydrogenation ability of MAO support would be very helpful for initiation of glycerol oxidation, in good agreement with the effect of the bases.<sup>[31,40]</sup>

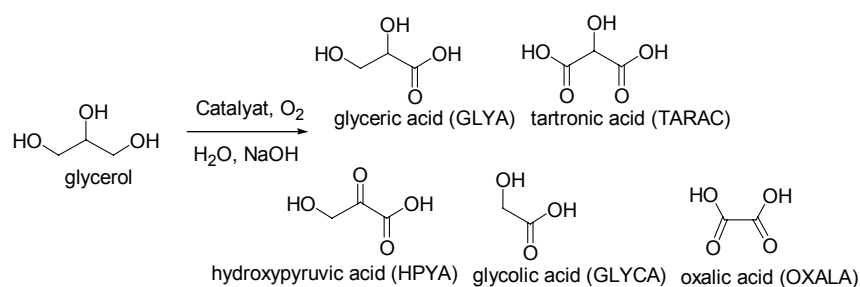
The product selectivity in glycerol oxidation is a critical factor for the choice of catalysts. Table 3 presents the catalytic conversion of glycerol and product selectivities over 0.7% Au/MAO, 0.9% Pd/MAO, and 0.7% Au-0.9% Pd/MAO catalysts. The catalytic products mainly consist of GLYA, TARAC, hydroxypyruvic

Table 2 TOFs of various catalysts in aerobic oxidation of glycerol<sup>a</sup>

Entry	Catalyst	Temperature/K	Oxygen pressure/MPa	NaOH/Glycerol (mol/mol)	TOF/h <sup>-1b</sup>	Ref.
1	0.7% Au/MAO	323	0.2	4	2300	
2	0.9% Pd/MAO	323	0.2	4	1840	
3	0.7% Au-0.9% Pd/MAO	323	0.2	4	9200	
4	1% Pd@Au/AC	323	0.3	4	6435	[27]
5	AuPd/C	333	1.0	2	8640	[33]
6	1% (Au-Pd)/C	343	0.3	4	981	[34]
7	0.7% Au/MAO	323	0.2	0	1100	
8	0.7% Au-0.9% Pd/MAO	323	0.2	0	2820	

<sup>a</sup> Reaction conditions: 3 mmol of glycerol, 10 mL of water, 12 mmol of NaOH, molar ratio of glycerol with metal (Au and Pd) at 3000;

<sup>b</sup> TOF numbers (h<sup>-1</sup>) were calculated on the basis of total loading of metals after reaction for 0.25 h.

**Table 3** Catalytic data of various catalysts in the aerobic oxidation of glycerol<sup>a</sup>

Entry	Catalyst	Conversion/%	Product selectivity/%					
			GLYA	TARAC	HPYA	GLYCA	OXALA	Others <sup>b</sup>
1	0.9% Pd/MAO	18.6	49.9	12.3	0.0	9.3	10.5	16.2
2	0.7% Au/MAO	85.2	66.2	10.0	8.4	5.8	4.6	5.0
3	0.7% Au-0.9% Pd/MAO	98.5	43.0	36.6	3.2	5.6	0.4	11.2

<sup>a</sup> Reaction conditions: 3 mmol of glycerol, 0.2 MPa of O<sub>2</sub>, 10 mL of water, 12 mmol of NaOH, molar ratio of glycerol with metal (Au and Pd) at 2000 under the temperature of 323 K for 2 h; <sup>b</sup> The by-products are dihydroxyacetone, glyoxylic acid, CO<sub>2</sub>, formic acid, and others.

acid (HPYA), glycolic acid (GLYCA), and oxalic acid (OXALA). Notably, 0.9% Pd/MAO catalyst shows low conversion (18.6%) and GLYA selectivity (49.9%, Table 3, Entry 1). However, 0.7% Au/MAO exhibits relatively high glycerol conversion (85.2%) and GLYA selectivity (66.2%, Table 3, Entry 2). These data are comparable with those of Au nanoparticles reported previously.<sup>[41]</sup> Interestingly, 0.7% Au-0.9% Pd/MAO catalyst exhibits very high conversion of glycerol, giving at 98.5%. In addition, relatively high selectivity for TARAC is obtained (36.6%, Table 3, Entry 3). This is quite different from the results in literature that GLYA was usually the major product with extremely low yield of TARAC in glycerol oxidation on Au, Au-Pd and Au-Pt catalyst.<sup>[4,27,33,34,36]</sup> Because TARAC is converted from further oxidation of GLYA, the high selectivity for TARAC is to suggest that 0.7% Au-0.9% Pd/MAO catalyst is very active.

## Conclusions

In summary, we have successfully designed and prepared bimetallic Au-Pd nanoparticles with rich edge and corner sites on MAO support (0.7% Au-0.9% Pd/MAO). This catalyst gives superior activities for the aerobic oxidation of benzyl alcohol to benzaldehyde. Very interestingly, this catalyst exhibits both high conversion of glycerol and high TARAC selectivity in the aerobic oxidation of glycerol. These results would be potentially important to develop of new catalysts for the production of fine chemicals.

## Acknowledgement

This work is supported by the National Natural Science Foundation of China (20973079 and U1162201) and the State Basic Research Project of China (2009CB623501).

## References

- [1] Hutchings, G. J. *J. Catal.* **1985**, *96*, 292.
- [2] Haruta, M.; Koboyashi, T.; Sano, H.; Yamada, N. *Catal. Lett.* **1987**, *16*, 405.
- [3] Herzing, A. A.; Kiely, C. J.; Carley, A. F.; Landon, P.; Hutchings, G. J. *Science* **2008**, *321*, 1331.
- [4] Villa, A.; Veith, G. M.; Prati, L. *Angew. Chem., Int. Ed.* **2010**, *49*, 4499.
- [5] (a) Ren, N.; Yang, Y. H.; Zhang, Y. H.; Wang, Q. R.; Tang, Y. *J. Catal.* **2007**, *246*, 215; (b) Wang, L.; Zhang, W.; Su, D.; Meng, X.; Xiao, F.-S. *Chem. Commun.* **2012**, *48*, 5476.
- [6] Abad, A.; Concepcion, P.; Corma, A.; Garcia, H. *Angew. Chem., Int. Ed.* **2005**, *44*, 4066.
- [7] (a) Zhang, X.; Shi, H.; Xu, B.-Q. *J. Catal.* **2011**, *279*, 75; (b) Wang, L.; Meng, X.; Xiao, F.-S. *Chin. J. Catal.* **2010**, *31*, 943.
- [8] Wang, L.; Wang, H.; Hapala, P.; Zhu, L.; Ren, L.; Meng, X.; Lewis, J. P.; Xiao, F.-S. *J. Catal.* **2011**, *281*, 30.
- [9] Su, F.-Z.; Liu, Y.-M.; Wang, L.-C.; Cao, Y.; He, H.-Y.; Fan, K.-N. *Angew. Chem., Int. Ed.* **2008**, *47*, 334.
- [10] Zhang, X.; Shi, H.; Xu, B.-Q. *Angew. Chem., Int. Ed.* **2005**, *44*, 7132.
- [11] Mori, K.; Hara, T.; Mizugaki, T.; Ebitani, K.; Kaneda, K. *J. Am. Chem. Soc.* **2004**, *126*, 10657.
- [12] Zhao, R.; Ji, D.; Lv, G. M.; Qian, G.; Yan, L.; Wang, X. L.; Suo, J. *S. Chem. Commun.* **2004**, 904.
- [13] Ma, C. Y.; Mu, Z.; Li, J. J.; Jin, Y. G.; Cheng, J.; Lu, G. Q.; Hao, Z. P.; Qiao, S. Z. *J. Am. Chem. Soc.* **2010**, *132*, 2608.
- [14] Yan, W.; Brown, S.; Pan, Z.; Mahurin, S. M.; Overbury, S. H.; Dai, S. *Angew. Chem., Int. Ed.* **2006**, *45*, 3614.
- [15] Zope, B. N.; Hibbits, D. D.; Neurock, M.; Davis, R. J. *Science* **2010**, *330*, 74.
- [16] Chen, M. S.; Kumar, D.; Yi, C. W.; Goodman, D. W. *Science* **2005**, *310*, 291.
- [17] Wang, L.; Meng, X. J.; Wang, B.; Chi, W. Y.; Xiao, F.-S. *Chem. Commun.* **2010**, *46*, 5003.
- [18] Zhang, Q. H.; Deng, W. P.; Wang, Y. *Chem. Commun.* **2011**, *47*, 9275.
- [19] Chen, Z.; Cui, Z.-M.; Fang, N.; Jiang, L.; Song, W.-G. *Chem. Commun.* **2010**, *46*, 6524.
- [20] Wang, L.; Meng, X.; Xiao, F.-S. *Chin. J. Catal.* **2010**, *31*, 943.
- [21] Min, B. K.; Friend, C. M. *Chem. Rev.* **2007**, *107*, 2709.
- [22] (a) Okumura, M.; Kitagawa, Y.; Haruta, M.; Yamaguchi, K. *Chem.*

- Phys. Lett.* **2001**, *346*, 163; (b) Si, R.; Flytzani-Stephanopoulos, M. *Angew. Chem., Int. Ed.* **2008**, *47*, 2884; (c) Fu, Q.; Weber, A.; Flytzani-Stephanopoulos, M. *Catal. Lett.* **2001**, *77*, 87; (d) Deng, W.; De Jesus, J.; Saltsburg, H.; Flytzani-Stephanopoulos, M. *Appl. Catal. A* **2005**, *291*, 126.
- [23] Lopez, N.; Janssens, T. V. W.; Clasuen, B. S.; Xu, Y.; Mavrikakis, M.; Bligaard, T.; Norskov, J. K. *J. Catal.* **2004**, *223*, 232.
- [24] Chen, M. S.; Goodman, D. W. *Science* **2004**, *306*, 5694.
- [25] Schubert, M. M.; Hackenberg, S.; van Veen, A. C.; Muhler, M.; Plzak, V.; Behm, R. J. *J. Catal.* **2001**, *197*, 113.
- [26] Dimitratos, N.; Villa, A.; Wang, D.; Porta, F.; Su, D. S.; Prati, L. *J. Catal.* **2006**, *244*, 113.
- [27] Wang, D.; Villa, A.; Porta, F.; Su, D. S.; Prati, L. *Chem. Commun.* **2006**, 1956.
- [28] Enache, D. I.; Edwards, J. K.; Landon, P.; Solsona-Espriu, B.; Carley, A. F.; Herzing, A. A.; Watanabe, M.; Liely, C. J.; Knight, D. W.; Hutchings, G. J. *Science* **2006**, *311*, 362.
- [29] Huber, G. W.; Iborra, S.; Corma, A. *Chem. Rev.* **2006**, *106*, 4044.
- [30] Chen, X. L.; Zheng, Y. G.; Shen, Y. C. *Chem. Rev.* **2007**, *107*, 1777.
- [31] Carrettin, S.; McMorn, P.; Johnston, P.; Griffin, K.; Kiely, C. J.; Hutchings, G. J. *Phys. Chem. Chem. Phys.* **2003**, *5*, 1329.
- [32] (a) Carrettin, S.; McMorn, P.; Hohnston, P.; Hutchings, G. J. *Chem. Commun.* **2002**, 696; (b) Fang, W.; Chen, J.; Zhang, Q.; Deng, W.; Wang, Y. *Chem. Eur. J.* **2011**, *17*, 1247.
- [33] Ketchie, W. C.; Murayama, M.; Davis, R. J. *J. Catal.* **2007**, *250*, 264.
- [34] Dimitratos, N.; Lopez-Sanchez, J. A.; Lennon, D.; Porta, F.; Prati, L.; Villa, A. *Catal. Lett.* **2006**, *147*, 108.
- [35] Miedziak, P. J.; Tang, Z.; Davies, T. E.; Enache, D. I.; Bartley, J. K.; Carley, A. F.; Herzing, A. A.; Kiely, C. J.; Taylor, S. H.; Hutchings, G. J. *J. Mater. Chem.* **2009**, *19*, 8619.
- [36] Villa, A.; Gaiassi, A.; Rossetti, I.; Nianchi, C. L.; van Benthem, K.; Veith, G. M.; Prati, L. *J. Catal.* **2010**, *275*, 108.
- [37] Kibler, L. A.; El-Aziz, A. M.; Hoyer, R.; Kolb, D. M. *Angew. Chem., Int. Ed.* **2005**, *44*, 2080.
- [38] Dimitratos, N.; Sanchez, J. A. L.; Morgam, D.; Carley, A.; Prati, L.; Hutchings, G. J. *Catal. Today* **2007**, *122*, 317.
- [39] Wang, L.; Zhang, J.; Meng, X.; Zheng, D.; Xiao, F.-S. *Catal. Today* **2011**, *175*, 404.
- [40] Garcia, R.; Besson, M.; Gallezot, P. *Appl. Catal. A* **1995**, *127*, 165.
- [41] Demirel-Gulen, S.; Lucas, M.; Claus, P. *Catal. Today* **2005**, *102*, 166.

(Zhao, X.)